https://dx.doi.org/10.22161/ijaers.5.7.7 *ISSN: 2349-6495(P) | 2456-1908(O)*

Optimal H Infinity Controller Applied to a Stewart Platform

Ricardo Breganon[1], Marcio A. F. Montezuma[2], Mateus M. de Souza[3], Rodrigo C. Lemes[3], Eduardo M. Belo[4]

[1]Federal Institute of Paraná, JACAREZINHO, PARANÁ, BRAZIL
Email: ricardo.breganon@ifpr.edu.br
[2]Federal Technologic University of Paraná, CORNÉLIO PROCÓPIO, PARANÁ, BRAZIL
Email: marcio.f.montezuma@gmail.com
[3]Federal Institute of São Paulo, SÃO CARLOS, SÃO PAULO, BRAZIL
Email: mateusmoreiradesouza@yahoo.com.br
Email: professorlemes@yahoo.com.br
[4]Engineering School of São Carlos - University of São Paulo, SÃO CARLOS, SÃO PAULO, BRAZIL
Email: belo@sc.usp.br

Abstract**—** *In recent years there has been great interest in studying parallel manipulators, mainly applied in flight simulators, with six degrees of freedom. The interest in parallel kinematic structures is motivated by its high stiffness and excellent positioning capability in relation to serial kinematic structures. This work presents the kinematic and dynamic modeling, design, development and identification of the parameters of motion platform with six degrees of freedom, electrically powered, for studies of flight simulators, is known as a Stewart Platform. It also presents the design of an H infinity controller with output feedback. The actuator model was obtained by a step voltage input to the engines and measuring its displacement by the encoders coupled, in each of the respective axes of the motors. Knowing the relation of motion transmission mechanism between the motor shaft and each actuator is obtained by the displacement rod from the rotation of motor which are measured by the corresponding encoder. The kinematics and dynamics platform's data compose the whole systems models simulations that are applied in the Stewart platform to validate the model and show the effectiveness of control techniques in which was applied to control the position and orientation of the platform were performed. An inertial sensor Xsens MTi-G measurement of the Euler angles of the platform was performed. The result obtained by the controller was satisfactory and illustrate the performance and robustness of the proposed methodology.*

Keywords**—** ***Stewart Platform, Flight Simulator, H infinity Controller, Position Controller, Orientation Controller.***

I. INTRODUCTION

Parallel structures have emerged in the '60s associated with flight simulators and, from the late '80s; parallel manipulators with rigid actuators have been used as the basis for simulations with various degrees of freedom. Stewart proposed a parallel structure with six degrees of freedom drawn from the adaptation of a flight simulator to a structure known since 1947 as Gough platform used to build a machine to test tires [1]. This structure became known as Stewart Platform [2].

Attitude and position control of Stewart platforms are real complex problems in several areas of study. The reference model for this mechanism can be split in two categories, hydraulic or electromechanical actuators [3, 4, 15]. For hydraulic actuators, depending on the load on the platform, it is necessary to model the system taking into account the dynamic characteristics of the hydraulic system and the platform. In the case of electromechanical actuators, where it has a gear ratio for conversion of angular velocity of the motor to linear velocity of the spindle. This transmission ratio plus friction can cause an inertial decoupling where the main dynamics can be considered only that of the actuator [18].

So, the main purpose of this paper is to present the platform that was developed for studies in control systems for flight simulators at the Laboratory of Airspace Control of the Engineering School of São Carlos of the University of São Paulo (Figure 1).

https://dx.doi.org/10.22161/ijaers.5.7.7 *ISSN: 2349-6495(P) | 2456-1908(O)*

Fig. 1: Stewart Platform

II. KINEMATIC MODELLING

The inverse kinematics of the parallel robot is to determine which length values to actuators that satisfy a known position and orientation of the end-effector. Compared with serial robots inverse kinematics which presents greater complexity than the direct kinematics, inverse kinematics in parallel robots is less complex than the direct kinematics. The inverse kinematics is used to generate trajectories [5, 16, 17]. However, a mathematical model that describes the six degrees of freedom of the end of the manipulator must describe the position and orientation of the same relative to some fixed reference.

This way the inverse kinematics begins to be defined from the rotation in X, Y and Z axes, which take the reference of the moving part of the platform (B) in the frame of its fixed base (A). These rotations are determined by Euler angles ∅, θ and ψ, where each of them is represented by the matrix (1), (2) and (3) respectively.

$$R(x,\emptyset) = \begin{bmatrix} 1 & 0 & 0 \\ 0 & \cos(\emptyset) & -sin(\emptyset) \\ 0 & sin(\emptyset) & \cos(\emptyset) \end{bmatrix} \quad (1)$$

$$R(y,\theta) = \begin{bmatrix} \cos(\theta) & 0 & sin(\theta) \\ 0 & 1 & 0 \\ -sin(\theta) & 0 & \cos(\theta) \end{bmatrix} \quad (2)$$

$$R(z,\psi) = \begin{bmatrix} \cos(\psi) & -sin(\psi) & 0 \\ sin(\psi) & \cos(\psi) & 0 \\ 0 & 0 & 1 \end{bmatrix} \quad (3)$$

In the design of a position and attitude control system of the movable platform that is located at the top base from the Stewart platform, becomes necessary to know the inverse kinematics of this mechanism [6]. The inverse kinematics uses the position and attitude of the movable platform with respect to the fixed platform to obtain the lengths of the actuators and can be addressed using tensor modeling [7] or modeling based on linear algebra [8, 14]. The modeling using linear algebra is presented in this paper.

The positions of the joints that connects the platforms to the actuators are defined in two coordinate systems [5]. A system with origin in the center of the fixed platform A and axis x_A pointing between joints 1 and 2 of the fixed platform, axis z_A perpendicular to the plane of the fixed platform pointing up and axis y_A completing the right-hand rule. The other system has the origin in the center of the movable platform B and axis x_B pointing between joints 1 and 2 of the movable platform, axis z_B perpendicular to the plane of the movable platform pointing upward and axis y_B completing the right-hand rule. The Figure 2 shows the definitions of the two coordinate systems.

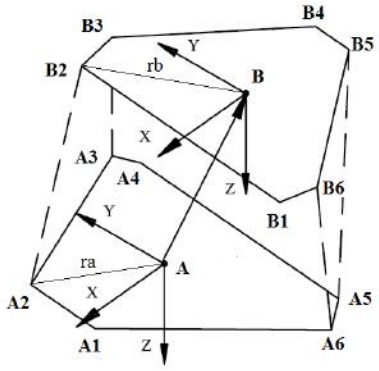

Fig. 2: Coordinate systems

The positions of the joints of the fixed and movable platforms coordinate systems centered at A_i and B_i respectively are expressed by Eqs. (4), (5), (6) and (7) as follows:

$$\{A_i\}^A = \{ra\cos(\Lambda a_i) \quad ra\,sin(\Lambda a_i) \quad 0\}^T = \{A_{i1} \quad A_{i2} \quad 0\}^T, \quad i = 1,2,\dots,6 \quad (4)$$

$$\{B_i\}^B = \{rb\cos(\Lambda b) \quad rbsin(\Lambda b_i) \quad 0\}^T = \{B_{i1} \quad B_{i2} \quad 0\}^T \quad (5)$$

$$\Lambda a_i = 60°i - \lambda a, \quad \Lambda b_i = 60°(i-1) + \lambda b, \quad i = 1,3,5 \quad (6)$$

$$\Lambda b_i = 60°(i-1) + \lambda b, \quad \Lambda a_i = 60°i - \lambda a, \quad i = 2,4,6 \quad (7)$$

where ra and rb are the radii of the circles centered at the center of the platform and contain the positions of the joints of the fixed and movable bases, respectively, and λa and λb are directors angles that help to define the positions of the joints of the fixed and movable platforms, respectively.

The vector representing the actuator in the fixed platform coordinate system $\{D_i\}^A$ is obtained using the Equation (8).

$$\{D_i\}^A = \{B_i\}^A - \{A_i\}^A \quad (8)$$

The vector representing the position of the joints of the movable platform in the fixed coordinate system is defined in Eq. (9)

https://dx.doi.org/10.22161/ijaers.5.7.7 *ISSN: 2349-6495(P) | 2456-1908(O)*

$$\{B_i\}^A = \{B\}^A + [T^{BA}] \times \{B_i\}^B = \begin{Bmatrix} x \\ y \\ z \end{Bmatrix} + \begin{Bmatrix} u_i \\ v_i \\ w_i \end{Bmatrix} \quad (9)$$

where $\{B\}^A$ is the vector that represents the position of the center of the movable platform in the coordinate system of the fixed platform and $[T^{BA}]$ is the transformation matrix of the movable coordinate system to the fixed coordinate system.

Using a sequence of three rotations, it is possible to obtain the transformation matrix $[T^{BA}]$. First, a rotation is applied around the axis x_B until axis y_B becomes parallel to the plane formed by x_A and y_A, and the rotation angle $\emptyset$ is called roll angle. Then, a rotation is applied around y_B until x_B is parallel to the plane formed by x_A and y_B, being the pitch angle θ. Finally, a rotation around z_B is applied until x_B is parallel to x_A, and this angle of rotation is the yaw angle ψ. The resulting matrix of the three rotations is shown in Equation (10). Where c is the cosine and s is the sine function.

$$R_B^A = \begin{bmatrix} c\psi\, c\theta & c\,\psi\, s\theta\, c\,\emptyset - s\psi\, c\emptyset & c\,\psi\, s\theta\, c\,\emptyset + s\psi\, s\emptyset \\ s\psi\, c\theta & s\psi\, s\theta\, s\emptyset + c\,\psi\, c\emptyset & s\psi\, s\theta\, c\,\emptyset - c\,\psi\, s\emptyset \\ -s\theta & c\,\theta\, s\emptyset & c\,\theta\, c\emptyset \end{bmatrix} \quad (10)$$

Finally, the vector representing the i-th actuator $\{D_i\}$ is obtained using information about the geometry of the Stewart Platform and defined the position and attitude of the movable platform. The module of this vector $|D_i|$ is equal to the length of the actuator it represents.

III. ACTUATOR MODEL

For the movable platform remains in the desired position and attitude relative to the fixed platform, it is necessary to control the lengths of the actuators by Inverse Kinematics. However all six electromechanical actuators were tested and mathematically modeled to represent the system dynamics.

These actuators consist of electric motors with gear transmissions for the ball screw. The motor is actuated by an electrical signal direct current with amplitude of up to 12 volts, through a power supply, and changes its direction of rotation by reversing the signal. To power the engine, a drive speed control brushed motors RoboClaw 2 is used, this drive receives a signal of 0 to 2 volt and converts it to an analog signal of -12 volts to 12 volts. An encoder of 1250 points per revolution was installed in the axis of rotation with the function to measure the revolutions number engines.

The acquisition system used for processing and transmission the data was dSPACE that sends 0 to 2 volts signal to the engine speed controller card and that receive the position signal of the encoders, which will be feedback in control loop. The dSPACE works with real-time interface, where the controller is fully programmable in block diagrams in Simulink.

The first test was used for the varying length of the actuator in relation to the number of engine revolutions. In this test, the engines were powered to increase the length of the actuators to some random positions along their courses, were then measured the number of rotations of the motor and the stroke length of the actuators. The Equations (11), (12), (13), (14), (15) and (16) show the Equations of the straight obtained for actuador 1 to actuator 6, respectively [19].

$$y_{c1} = 0{,}00081315P + 7{,}8485 \quad (11)$$
$$y_{c2} = 0{,}00081329P + 11{,}6446 \quad (12)$$
$$y_{c3} = 0{,}00081225P + 9{,}8059 \quad (13)$$
$$y_{c4} = 0{,}00081201P + 11{,}1418 \quad (14)$$
$$y_{c5} = 0{,}00081207P + 9{,}7201 \quad (15)$$
$$y_{c6} = 0{,}00081252P + 9{,}4454 \quad (16)$$

where y_c is the length of stroke of the actuators in millimeters and P is the number of rotations of the motor measured in the encoder points.

The dynamics characteristics actuator's response was obtained in the second experiment, for greater reliability, the tests were performed three times and made the average of these results. In this test were applied step inputs voltage to the motor of the electromechanical actuator and the variation of the stroke of the actuator was obtained by reading the encoder, together with Equations (11) (12) (13) (14) (15) and (16). The Figure 3 represents the variations of the length of stroke of the actuator 1, when applied signals 4, -4, 6, -6, 8, -8, 10, -10, 12, -12 of volts. This procedure was repeated in the same way for all the actuators of the Stewart Platform. It can be seen that the actuators lengths increases with positive signals whilst their lengths decrease with negative signals while the voltage signal is applied and stopping only at the limits of course.

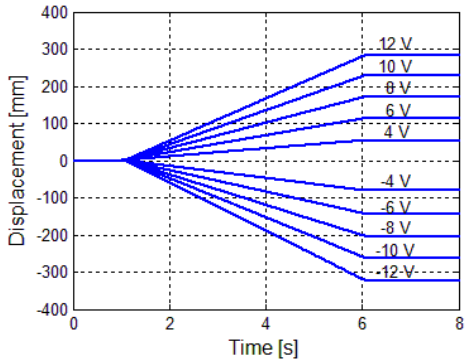

Fig. 3: Stroke length variations of the actuator 1

During the experiment was observed that the actuators, although having the similar physical properties and be of the same manufacturer, showed different responses to the same voltage signal applied. Therefore it was necessary identification and modeling for each of the six electromechanical actuators. The Figure 4 shows the variations in the length found for a step input signal 12V

https://dx.doi.org/10.22161/ijaers.5.7.7 *ISSN: 2349-6495(P) | 2456-1908(O)*

applied to the actuators 1 to 6, respectively. It can also be observed that the actuators behavior with relations to the negative voltages and the positive voltage are not symmetrical, and also as occurred for positive voltages, the actuators showed different responses to each other for the same input. The Figure 5 shows the variation of length of all the actuators to the voltage -12V.

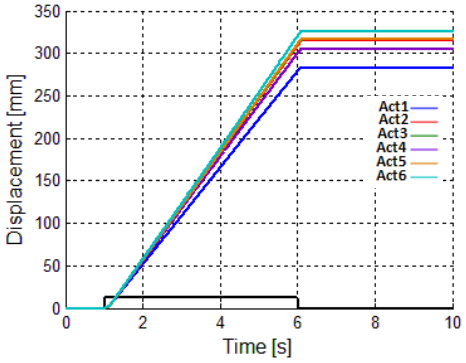

Fig. 4: Lengths variations for a step input signal 12V

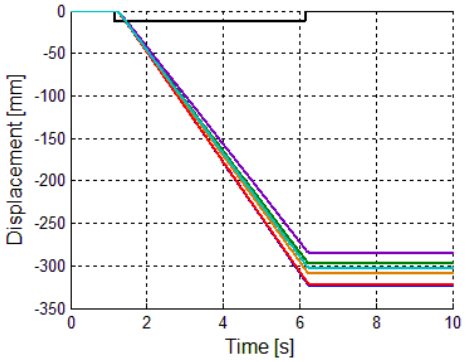

Fig. 5: Lengths variations for a step input signal -12V

Short information to the dynamic response of the actuators can be obtained using the length actuators variation to the step input, but using the responses of velocities forward and return actuators as shown in Figure 6 it can be observed that the velocity shows a stable response to a step input in all voltage levels analyzed. So we worked with the velocity to survey the dynamics of actuators.

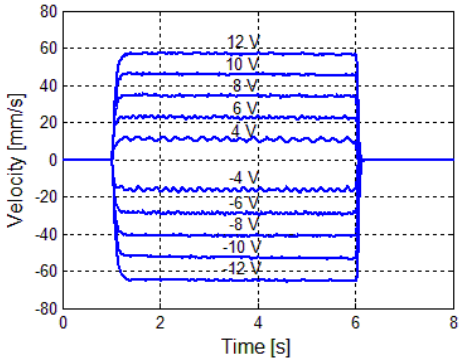

Fig. 6. Velocities of the actuator 1

The actuators has different speeds, a problem that causes each actuator must be treated independently. The Figure 7 shows the forward speed of 6 actuators tested where you can see the difference in behavior of each of the actuators. Negative voltages were also applied in order to check the recoil velocity of the actuators. The Figure 8 shows the speed of the six actuators for voltage -12V, also is possible to observe that the actuators behave differently between the advance and retreat of the actuators lengths.

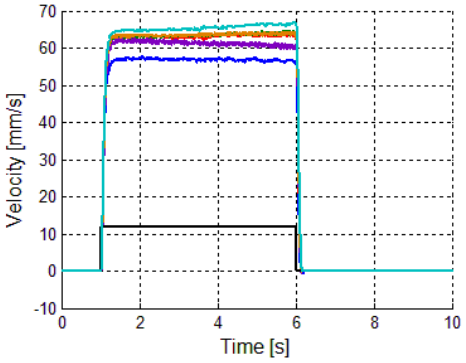

Fig. 7: Velocities of the six actuators for 12V

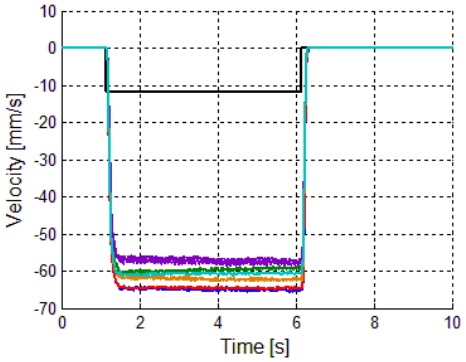

Fig. 8: Velocities of the six actuators for -12V

Based on the velocity response in the application step of inputs 4, -4, 6, -6, 8, -8, 10, -10, 12, -12 volts, shown in Figures 6, it was observed that the system displays a response without overshoot, but has a noise characteristic oscillation system. It can be argued that this response is typical of a system of first order but at least responding to noise regime. Where as the model of a complex formed by electric motor and mechanical parts of an actuator can be approximated by a second order dynamic system, so it was decided to use as a simplified model for the transfer function of the velocity of the electromechanical actuator by signal voltage, a system of second order, as shown by Equation (17).

$$\frac{Y(s)}{U(s)} = \frac{k}{(s+a)^2} \tag{17}$$

where k is the gain, is the double pole of the second order system, and $\frac{Y(s)}{U(s)}$ is the Laplace transform of the stroke speed and the voltage signal, respectively.

The characteristics of the system Equation 17 can be obtained by comparing the response velocity of actuator

https://dx.doi.org/10.22161/ijaers.5.7.7 *ISSN: 2349-6495(P) | 2456-1908(O)*

stroke with the characteristics of the response of a second order system to a step input [9, 10].

Because of the presence of noise on the response velocity of the actuators courses, were used average values, taken from three tests conducted for all levels of input signals, as shown in Table 1.

In this experiment it was observed that the actuators have dead zone (Dz), as shown in Table 2. In other words, this voltage range does not change the stroke length actuators. This characteristic makes instead of using the value of the entry step in the calculations of Equations (17) and (18), we use the effective value of the step input, which is the difference between the value of the step input and dead zone.

Table.1: Mean Velocity of actuators

Mean of velocities of actuators in a regime (mm/s)						
Volts	Act 1	Act 2	Act 3	Act 4	Act 5	Act 6
4V	11,4	17,3	15,2	11,4	16,3	17,8
6V	23,0	29,0	27,6	24,4	28,5	29,9
8V	34,6	40,8	39,8	37,3	40,4	42,0
10V	45,9	52,2	52,0	49,6	52,1	54,0
12V	57,1	63,5	63,5	61,5	63,6	65,4
-4V	- 16,4	- 17,6	- 14,7	- 12,8	- 14,9	-15,2
-6V	- 28,9	- 29,5	- 26,5	- 25,1	- 27,0	- 26,8
-8V	- 40,9	- 41,2	- 37,8	- 36,8	- 38,9	- 38,3
-10V	- 53,1	- 52,8	- 49,0	- 47,5	- 50,8	- 49,9
-12V	- 65,2	- 64,7	- 59,7	- 57,5	- 62,2	- 60,8

Table.2: Values of dead zone

	Act1	Act2	Act3	Act4	Act 5	Act 6
Dz+	1,98V	0,97V	1,45V	2,12V	1,19V	0,99V
Dz -	-1,27V	-0,99V	-1,3V	-1,56V	-1,45V	-1,31V

As the stroke length of the actuator is the integral of the velocity of course, the stroke length transfer function of the effective voltage signal can be represented by Equation (18), where X(s) is defined as the change in length actuator stroke.

$$\frac{X(s)}{U(s)} = \frac{1}{s} \times \frac{k}{(s+a)^2} = \frac{A_0}{s} + \frac{A_1}{(s+a)} + \frac{A_2}{(s+a)^2} \quad (18)$$

where A_0, A_1 and A_2 can be obtained using the partial fraction expansion theorem of Heaviside, shown in Equations (19), (20) and (21). The advantage of using a partial fraction expansion is that the individual terms, which result from this expansion in the form of partial fractions, are very simple functions [10].

$$A_0 = \frac{k}{a^2} \quad (19)$$

$$A_1 = -\frac{k}{a^2} \quad (20)$$

$$A_2 = -\frac{k}{a} \quad (21)$$

Applying the inverse transform Laplace into Equation (18), the stroke length of the actuator has the answer in Equation (22). Replacing terms of Equations (19), (20) and (21) into Equation (22) are obtained the Equations (23) and (24).

$$r(t) = A_0 + A_1 e^{-at} + A_2 t e^{-at} \quad (22)$$

$$r(t) = \frac{k}{a^2} - \frac{k}{a^2} e^{-at} - \frac{k}{a} t e^{-at} \quad (23)$$

$$r(t) = \frac{k}{a^2}(1 - e^{-at} - ate^{-at}) \quad (24)$$

In order to identify the k and a terms the following procedure was used: first identified the time of application of a step voltage input to the stroke speed reaches 60% of its value regime. These values can be substituted in Equation (24) and then the resulting Equation (25) is obtained.

$$0{,}6 = 1 - e^{-at_{60\%}} - at_{60\%} e^{-at_{60\%}} \quad (25)$$

However, Equation (25) does not present direct solution to obtain the value of a, so it was necessary to use numerical methods for the identification of the parameter. Equation (25) was rewritten in the form of Equation (26), to then create a function F that depends on the a.

$$\underbrace{e^{-at_{60\%}} + at_{60\%} e^{-at_{60\%}}}_{F} = 0{,}4 \quad (26)$$

Then we used the linearization of the function F by Taylor polynomial shown in Equation (27).

$$F(a) = F(a_0) + \frac{dF(a_0)}{da}(a - a_0) \quad (27)$$

An iterative method in which the value of the a initialized as shown in Equation (28) is then calculated value of the function F and its derived using Equation (26), was used to calculate a new value of a using the Equation (29). This procedure was used so that the function F have lower error than 0.001 for the current value of a.

$$a = \frac{\ln(0{,}4)}{t_{60\%}} \quad (28)$$

$$a = \frac{F(a)}{dF} + a_0 - \frac{F(a)}{dF} \quad (29)$$

Identified the value of the parameter a, it was necessary to identify the value of k, using it for the Equation (24). Therefore, to find the value of k was used in Equation (30) which is the value in a regime the velocity of the actuator stroke. The values obtained for k and each actuator are shown in the Table 3.

$$Vr = \frac{k}{a^2} \quad (30)$$

https://dx.doi.org/10.22161/ijaers.5.7.7 *ISSN: 2349-6495(P) | 2456-1908(O)*

Table.3: Values of k and a

	Act1	Act 2	Act 3	Act 4	Act 5	Act 6
k	7137	7345	7269	6928	6360	8513
a	34,23	34,93	34,55	33,35	32,28	34,32

Thus we obtain the transfer functions that represent the dynamics of each actuator, shown in Equations (31), (32), (33), (34), (35) and (36).

$$R = \frac{7137}{s(s+34{,}23)^2} = \frac{7137}{s^3 + 68{,}46s^2 + 1171s} \quad (31)$$

$$R = \frac{7345}{s(s+34{,}93)^2} = \frac{7345}{s^3 + 69{,}86s^2 + 1220s} \quad (32)$$

$$R = \frac{7269}{s(s+34{,}55)^2} = \frac{7269}{s^3 + 69{,}1s^2 + 1194s} \quad (33)$$

$$R = \frac{6928}{s(s+33{,}35)^2} = \frac{6928}{s^3 + 66{,}7s^2 + 1112s} \quad (34)$$

$$R = \frac{6360}{s(s+32{,}28)^2} = \frac{6360}{s^3 + 64{,}56s^2 + 1042s} \quad (35)$$

$$R = \frac{8513}{s(s+34{,}32)^2} = \frac{8513}{s^3 + 68{,}64s^2 + 1178s} \quad (36)$$

IV. H INFINITY CONTROL

To Real systems are subject to different types of disturbances. Uncertainties in the mathematical model of the system can be modeled as a disturbance in the nominal model. These uncertainties have different origins, it can be highlighted: the existence of errors in the values of model parameters or the values of the parameters are unknown, the parameters in linear model may vary due to nonlinearities or variation of the operating point; associated errors measuring instruments and the structure of the model at high frequencies is not known, resulting that the sum of all uncertainties can overcome the personal gain of the plants.

The problem of H infinity control was first formulated by G. Zames. H infinity refers in the space to the transfer function own and stable. The design of H infinity control is designed in the frequency domain in the context of optimizing the space of transfer functions given objective function in terms of the standard H infinity. The H infinity norm of a transfer function is defined as shown in the Equation (37) [11].

$$\|G(jw)\|_\infty = sup_w |G(jw)| \quad (37)$$

The design of H infinity control considers the worst case operation and involves the minimization of the peak of the matrix transfer function in the scalar case this would minimize peak of the transfer function in the frequency domain and in multiple inputs and outputs case would be to minimize the maximum singular value represented by this norm.

The term H is the Hardy space where the space of functions with complex matrices, name space due to the mathematical Hardy. And the infinite term comes from the use of the infinity norm and the infinity symbol limit of Hp norm when p tends to infinity. Figure 9 shows the standard block representation where P (s) is the increased transfer function.

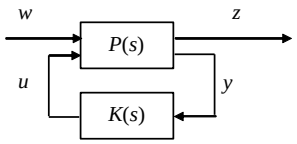

Fig. 9: Standard block representation

From the diagram above, results in:

$$\begin{bmatrix} z \\ y \end{bmatrix} = P \begin{bmatrix} w \\ u \end{bmatrix} = \begin{bmatrix} P_{11} & P_{12} \\ P_{21} & P_{22} \end{bmatrix} \begin{bmatrix} w \\ u \end{bmatrix}, u = Ky \quad (38)$$

Then the transfer function between the external input w and regulated output z. Substituting u in the Equation y

$$y = P_{21}w + P_{22}Ky \quad (39)$$

$$y = (I - P_{22}K)^{-1}P_{21}w \quad (40)$$

And, we can write:

$$u = Ky = K(I - P_{22}K)^{-1}P_{21}w \quad (41)$$

Finally, replacing u in the Equation z it result at

$$z = P_{11}w + P_{12}K(I - P_{22}K)^{-1}P_{21} \quad (42)$$
$$= [P_{11} + P_{12}K(I - P_{22}K)^{-1}P_{21}]w$$
$$z = T_{zw}w, \; T_{zw} = P_{11} + P_{12}K(I - P_{22}K)^{-1}P_{21} \quad (43)$$

The augmented plant in the form of state space is of the form

$$\dot{x} = Ax + B_1w + B_2u \quad (44)$$
$$z = C_1x + D_{11}w + D_{12}u \quad (45)$$
$$y = C_2x + D_{21}w + D_{22}u \quad (46)$$

A. Weighting Functions

In the H infinity design in general weighting functions are employed to specify the stability and performance of the system. Understanding the effects of these functions on the control system is crucial for modeling specifications. A typical model for design, called augmented plant is shown in Figure 10. The weighting functions W_1, W_2 and W_3 reflect the value specified error for the regime, limitations of the control signal and the stability condition, respectively. The standard method H infinity output feedback is used to stabilize the system. The standard H infinity control problem is formulated in terms of finding a controller K, if one exists, such that for a given $\gamma > 0$.

$$\|T_{zw}\|_\infty = \left\| \begin{matrix} W_1S \\ W_2KS \\ W_3T \end{matrix} \right\|_\infty \quad (47)$$

https://dx.doi.org/10.22161/ijaers.5.7.7 ISSN: 2349-6495(P) | 2456-1908(O)

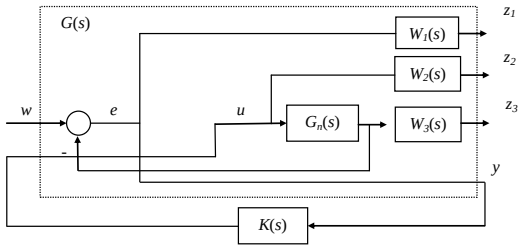

Fig. 10: Augmented plant

The weighting functions represent the design specifications and modeling errors, restricting Z_1, Z_2 and Z_3 of augmented plant output, as shown below:

The $W_1(s)$ function is a limiting factor for the sensitivity function S, and should reflect the rejection of external disturbances, considering the error signal Z_1 system and tolerance to variations in the plant. The sensitivity S should take low value, especially at low frequencies. Therefore, W_1 function, which reflects the performance specifications, must submit a high value at low frequencies.

The $W_2(s)$ function weighs Z_2, that is the control signal, and must have sufficient gain capacity to limit the input control an acceptable range, avoiding the saturation of the actuator. However, a high gain can deteriorate the performance, and this commitment must be taken into account. The W_2 function is linked to limitations in the input signal of the plant G_n such as maximum voltages or currents supported by the plant.

The $W_3(s)$ function weighs Z3 namely the plant output G_n, and should minimize the peak of the complementary sensitivity function T system, reducing the oscillations and ensuring stability [11].

Thus we have the same sensitivity function $S = (I + GK)^{-1}$, the complementary sensitivity function $T = I - S$ and the sensitivity function of the controller $C = KS$.

B. Synthesis Controller

The H infinity control in this section is based on a compensator project and an observer whose solutions are obtained by two algebraic Riccati Equations and results in a controller with the same number of states of the plant [12]. P(s) is the state-space realization of an augmented plant, according to Equation (48).

$$P(s) = \begin{bmatrix} A & B_1 & B_2 \\ C_1 & D_{11} & D_{12} \\ C_2 & D_{21} & D_{22} \end{bmatrix} \quad (48)$$

Consider the state space representation of the augmented system, including the dynamics of the weighting functions, is given by:

$$\begin{bmatrix} \dot{x} \\ z \\ y \end{bmatrix} = \begin{bmatrix} A & B_1 & B_2 \\ C_1 & 0 & D_{12} \\ C_2 & D_{21} & 0 \end{bmatrix} \begin{bmatrix} x \\ w \\ u \end{bmatrix} \quad (49)$$

The following hypotheses are considered in H infinity problems [12]:

(A, B_2, C_2) is stabilizable and detectable;

D_{12} *e* D_{21} have (post) complete;

$\begin{bmatrix} A - j\omega I & B_2 \\ C_1 & D_{12} \end{bmatrix}$ has complete column post for all ω;

$\begin{bmatrix} A - j\omega I & B_1 \\ C_2 & D_{21} \end{bmatrix}$ has complete line post for all ω;

$D_{11} = 0$ *e* $D_{22} = 0$;

$D_{12} = \begin{bmatrix} 0 \\ I \end{bmatrix}$ *e* $D_{21} = [0 \quad I]$;

$D_{12}^T C_1 = 0$ *e* $B_1 D_{21}^T = 0$ and

(A, B_1) is stabilizable and (A, C_1) is detectable.

The following Riccati Equations are associated with the H infinity problem:

$$A^T X + XA + C_1^T C_1 + X(\gamma^{-2} B_1 B_1^T - B_2 B_2^T)X = 0 \quad (50)$$

so that $Re\ \lambda_i[A + (\gamma^{-2} B_1 B_1^T - B_2 B_2^T)X] < 0, \forall i$ and

$$YA^T + AY + B_1 B_1^T + Y(\gamma^{-2} C_1^T C_1 - C_2^T C_2)Y = 0 \quad (51)$$

so that $Re\ \lambda_i[A + Y(\gamma^{-2} C_1^T C_1 - C_2^T C_2)] < 0, \forall i$.

Given the hypotheses outlined previously, the Equations of Ricatti admit stabilizing solutions $X\infty$ and $Y\infty$, and $\rho(X\infty Y\infty) < \gamma^2$, with $\rho(\cdot)$ the spectral radius, then there is a controller that internally stabilizes system $u = Ky$ so that the norm of the transfer function of closed loop $T_{zw} = P_{11} + P_{12}K(I - P_{22}K)^{-1}P_{21}$ is small, this is $\|T_{zw}\| < \gamma$, with γ a scalar positive [13]. The controller is given by:

$$\begin{bmatrix} \dot{x}_C \\ u \end{bmatrix} = \begin{bmatrix} A_C & B_C \\ C_C & 0 \end{bmatrix} \begin{bmatrix} x_C \\ y \end{bmatrix} \quad (52)$$

and

$$A_C = A + \gamma^{-2} B_1 B_1^T X_\infty + B_2 F_\infty + Z_\infty L_\infty C_2 \quad (53)$$

$$B_C = -Z_\infty L_\infty \quad (54)$$

$$C_C = F_\infty = -B_2^T X_\infty \quad (55)$$

$$L_\infty = -Y_\infty C_2^T \quad (56)$$

$$Z_\infty = (I - \gamma^{-2} X_\infty Y_\infty)^{-1} \quad (57)$$

V. RESULT EXPERIMENTAL AND DISCUSSION

An input step of 15 ° in angle ϕ was applied, representing the movement of roll in the Stewart Platform. The Figure 11 shows the movement of all actuators, stabilizing at the required position. The Figure 12 shows the control action to move the platform to the desired orientation, to provide increased stroke length of the actuator is possible to observe what happened cutting the signal voltage of 12V, set by the saturator. The Figure 13 shows that the error tended to zero.

https://dx.doi.org/10.22161/ijaers.5.7.7 *ISSN: 2349-6495(P) | 2456-1908(O)*

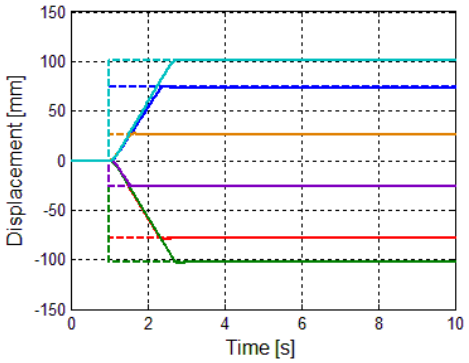

Fig. 11: Responses for 15º in ϕ

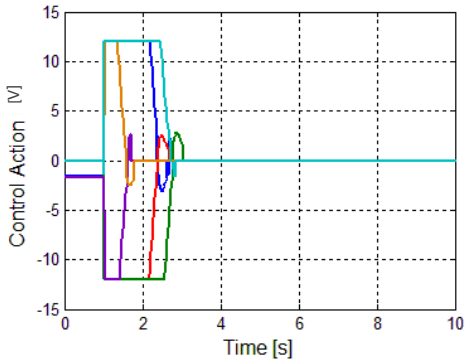

Fig. 12: Control Actions for 15º in ϕ

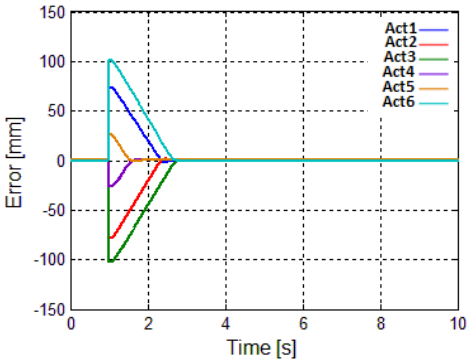

Fig. 13: Error for 15º in ϕ

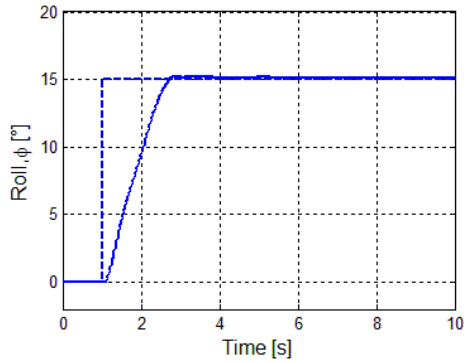

Fig. 14: Input step for 15º in roll

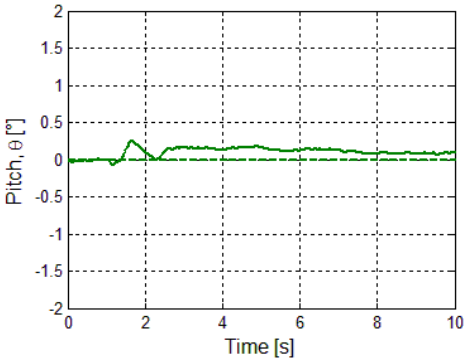

Fig. 15: Pitch for 15º in roll

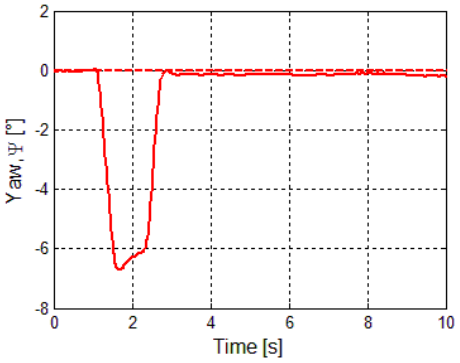

Fig. 16: Yaw for 15º in roll

The Figure 14 shows the angle ϕ for reading the input step 15º. You can see that the controller could converge to the desired orientation. The Figure 15 shows the reading of the angle θ remains near zero degrees, and the Figure 16 shows the reading angle ψ with a variation in the beginning of the step input, and thereafter tended to zero, as desired.

VI. CONCLUSION

For all this, it can be concluded that the methodology used for the identification of parameters and modeling the actuators showed good accuracy, introducing a mathematical model with the characteristics design of the next actual platform.

The experimental results show that the H infinity controller with output feedback can work well at different working conditions, being effective for the control of position and orientation of the actual model of the Stewart Platform. Small errors in result of yaw were observed during experiments to control orientation may be assigned by the existing clearances in the joints, the constructive differences of actuators, plus the error of inaccuracy of the sensor.

https://dx.doi.org/10.22161/ijaers.5.7.7 *ISSN: 2349-6495(P) | 2456-1908(O)*

ACKNOWLEDGEMENTS

This work was supported by CNPq (National Council for Scientific and Technological Development).

REFERENCES

[1] STEWART, D. (1965). A platform with six degrees of freedom. *Proceedings of Institution of Mechanical Engineers*, Part 1, v.180, n.15, p.371-86.

[2] DASGUPTA, B.; MRUTHYUNJAYA, T.S. (2000) The Stewart Platform Manipulator: a review. Mechanism and Machine Theory 35. 15-40 p. Pergamon.

[3] QIANG, W., JUAN, C. AND ZHIYOUNG, T., (2008). "Study of sliding mode control for Stewart Platform based on simplified dynamic model". In The IEEE International Conference on Industrial Informatics – INDIN 2008. Daejeon, Korea.

[4] RÉMILLARD, V., BOUKAS, EL-K., "Gough-Stewart Platform Control: A fuzzy control approach". In *Annual Conference of the North American Fuzzy Information Processing Society*. Montreal, Canada.

[5] GONZALEZ ACUÑA, Hernán (2009). Projeto mecatrônico de uma plataforma Stewart para simulação dos movimentos nos navios. 112 p. Dissertação (Mestrado em Engenharia Mecânica), Universidade Federal do Rio de Janeiro, COPPE, Rio de Janeiro.

[6] TRAVI, Alexandre Back e (2009). Plataforma de Stewart Acionada por Cabos. 114 p. Dissertação (Mestrado em Engenharia Mecânica), Instituto Militar de Engenharia, - Rio de Janeiro.

[7] ZIPFEL, P. H., (2000). "Modeling and simulation of aerospace vehicle dynamics". Reston, VA: American Institute of Aeronautics and Astronautics. 551p.

[8] NGUYEN, C. C. et al. (1993). Adaptive control of a Stewart Platform-Based manipulator. Journal of Robotic Systems, v.10, n.5, p.657-87.

[9] D'AZZO, J. J.; HOUPIS, H. C. (1995). *Linear control system analysis and desing: conventional and modern*. 3rd ed., New York, McGraw Hill Publishing Company.

[10] OGATA, K. (2003) Engenharia de Controle Moderno. 4ª Ed. São Paulo, Pearson: Prentice-Hall.

[11] OLIVEIRA, V.A.; AGUIAR, M.L.; VARGAS, J.B. (2005) Sistemas de Controle – Aulas de Laboratório. Departamento de Engenharia Elétrica. EESC/USP, São Carlos, SP.

[12] DOYLE, J. C. et al (1989). State-space solutions to standard H2 and H∞ control problems, IEEE Transactions on Automatic Control 34(8):831–847 p.

[13] ZHOU, K.,;DOYLE, J. C. and GLOVER, K. (1995). Robust and Optimal Control, Upper Saddle River: Prentice Hall.

[14] HUANG, X., HANG, Z., HE, G. and TAN, X., (2010). "An efficient algebraic method for direct kinematics of the 5-6 Stewart Platform". In *2010 2nd International Asia Conference on Informatics in Control, Automation and Robotics*. Wuhan, China.

[15] FICHTER, E. F. (1986). A Stewart Platform-Based manipulator: general theory and practical construction. *International Journal of Robotics and Research*, v.5, n.2, p.157-82.

[16] MERLET, J.P. (2000). *Paralell robots*. Dordrecht: Kluwer Academic Publishers.

[17] ROSARIO, J.M. et al (2007) Control of a 6-DOF Parallel Manipulator through a Mechatronic Approach *Journal of Vibration and Control*, 1431–1446 p. Publications Los Angeles, London, New Delhi, Singapore.

[18] MONTEZUMA, M. A. F. (2010). Metodologia para identificação e controle de um protótipo de uma plataforma de movimento com 2 G.D.L. 169 p. Tese (Doutorado em Engenharia Mecânica), Escola de Engenharia de São Carlos, Universidade de São Paulo, São Carlos.

[19] BREGANON, Ricardo, et al (2013). Attitude and Position Tracking System for a 6-6 Stewart Platform. In: 22nd International Congress of Mechanical Engineering, Ribeirão Preto. COBEM.